



Article

Structurally Diverse Diterpenes from the South China Sea Soft Coral *Sarcophyton trocheliophorum*

Yu-Ting Song^{1,2}, Dan-Dan Yu⁴, Ming-Zhi Su⁴, Hui Luo⁵, Jian-Guo Cao², Lin-Fu Liang^{3,*}, Fan Yang^{2,*} and Yue-Wei Guo^{1,*}

¹ State Key Laboratory of Drug Research, Shanghai Institute of Materia Medica, Chinese Academy of Sciences, 555 Zu Chong Zhi Road, Zhangjiang Hi-Tech Park, Shanghai 201203, China

² College of Life Sciences, Shanghai Normal University, 100 Guilin Road, Shanghai 200234, China

³ College of Materials Science and Engineering, Central South University of Forestry and Technology, 498 South Shaoshan Road, Changsha 410004, China

⁴ Shandong Laboratory of Yantai Drug Discovery, Bohai rim Advanced Research Institute for Drug Discovery, Yantai 264117, China

⁵ Key Laboratory of Zhanjiang for Research and Development Marine Microbial Resources in the Beibu Guif Rim, Marine Biomedical Research Institute, Guangdong Medical University, Zhanjiang 524023, China

* Correspondence: lianglinfu@csuft.edu.cn (L.-F.L.); bayer@shnu.edu.cn (F.Y.); ywguo@simm.ac.cn (Y.-W.G.)

Abstract: The present investigation of the South China Sea soft coral *Sarcophyton trocheliophorum* resulted in the discovery of six new polyoxygenated diterpenes, namely sartrocheliols A–E (**1**, **3**, **5–8**) along with four known ones, **2**, **4**, **9**, and **10**. Based on extensive spectroscopic data analysis, sartrocheliol A (**1**) was identified as an uncommon capnosane diterpene, while sartrocheliols B–E (**3**, **5–8**) were established as cembrane diterpenes. They displayed diverse structural features not only at the distinctly different carbon frameworks but also at the various types of heterocycles, including the epoxide, γ -lactone, furan, and pyran rings. Moreover, their absolute configurations were determined by a combination of quantum mechanical-nuclear magnetic resonance (QM-NMR) approach, modified Mosher's method, and X-ray diffraction analysis. In the anti-tumor bioassay, compound **4** exhibited moderate cytotoxic activities against A549, H1975, MDA-MB-231, and H1299 cells with the IC₅₀ values ranging from 26.3 to 47.9 μ M.

Keywords: soft coral; *Sarcophyton trocheliophorum*; capnosane; cembrane; absolute configuration; anti-tumor activity



check for updates

Citation: Song, Y.-T.; Yu, D.-D.; Su, M.-Z.; Luo, H.; Cao, J.-G.; Liang, L.-F.; Yang, F.; Guo, Y.-W. Structurally Diverse Diterpenes from the South China Sea Soft Coral *Sarcophyton trocheliophorum*. *Mar. Drugs* **2023**, *21*, 69. <https://doi.org/10.3390/md21020069>

Academic Editors: Vassilios Roussis, Bin-Gui Wang and Haofu Dai

Received: 15 December 2022

Revised: 17 January 2023

Accepted: 17 January 2023

Published: 20 January 2023



Copyright: © 2023 by the authors. Licensee MDPI, Basel, Switzerland. This article is an open access article distributed under the terms and conditions of the Creative Commons Attribution (CC BY) license (<https://creativecommons.org/licenses/by/4.0/>).

1. Introduction

A fairly large variety of bioactive secondary metabolites have been found in the soft corals of the genus *Sarcophyton* [1–4]. Over the past few decades, about 20 *Sarcophyton* species have been chemically investigated and more than 500 secondary metabolites have been identified. Based on their structural types, these metabolites could be classified into terpenes [2], steroids [3,5–7], quinones [8,9], prostaglandins [10,11], ceramides [12,13], and other miscellaneous compounds [8,14,15]. As reported in the literature, terpenes have dominated the chemical profile of the genus *Sarcophyton* [2,16]. Moreover, terpenes display rich structural diversities, which could be further categorized as sesquiterpenes [17–19], diterpenes [20–24], and biscembranoids [21,25–28]. Moreover, these metabolites exhibit a wide spectrum of biological activities, including anti-angiogenic [17], antimicrobial [27,29], cytotoxic [29,30], anti-inflammatory [27,31], immunomodulatory [25], antifouling [8,32], and neuroprotective [33,34] effects. The intriguing chemical and biological properties of terpenes have led to extensive attention from global researchers [35].

In the last decades, we systematically carried out chemical and biological studies on South China Sea marine fauna and flora [36]. As a result, numerous terpenes with complex structures, some of which possessed unprecedented carbon frameworks, were found from

the genus *Sarcophyton* [20,37,38]. During our continuous research, we frequently encountered the soft coral *Sarcophyton trocheliophorum*, one productive species belonging to the above-mentioned genus. Previously, our group disclosed a vast array of diterpenes with four skeletons, and these metabolites showed a broad spectrum of pharmacological activities such as protein tyrosine phosphatase 1B (PTP1B) inhibitory, antitumor, antibacterial and neuroprotective activities [39]. It was interesting to notice that the chemical profiles of diterpenes from the title soft corals varied upon temporal variations and geographical distributions. The samples collected in Yalong Bay, Hainan Island, South China Sea in February 2006 yielded diterpenes with an unprecedented carbon framework [37] together with sarsolenane, capnosane, and cembrane skeletons [39]. However, the specimen collected in the same water but in May 2006 only yielded cembrane diterpenes [40]. Of more interest, the soft corals collected from another different region, Ximao Island, South China Sea, merely afforded the cembranoids [41]. These findings probably reflected the existence of different metabolic processes in different seasons and inhabiting environments, which needs to be further investigated.

In order to obtain more evidence to disclose that the diterpenoid profile of the title animals was influenced by temporal variations, we made a new collection of *S. trocheliophorum* from Ximao Island. In the current study, six new polyoxygenated diterpenes, namely sartrocheliols A–E (1, 3, 5–8), and four known related analogs 2, 4, 9, and 10 were obtained (Figure 1). These diterpenes displayed two distinctly different carbon frameworks: capnosane and cembrane, the former of which has rarely been found in soft corals. Meanwhile, various types of heterocycles, including the epoxide, γ -lactone, furan, and pyran rings were incorporated in their macrocyclic skeletons. Herein, we report the detailed structural elucidation of these isolates from the title soft corals, especially the challenging stereochemistry determination of the new compounds, which was dissolved by a combination of quantum mechanical-nuclear magnetic resonance (QM-NMR) approach, modified Mosher's method, and X-ray diffraction analysis. In addition, their biological evaluations including cytotoxicity against a panel of cancer cells and antibacterial against an array of bacteria are described.

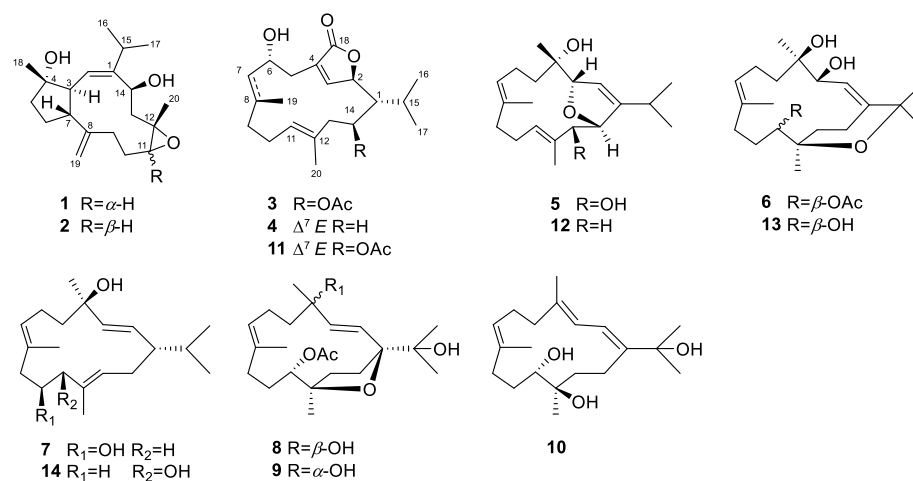


Figure 1. The chemical structures of compounds 1–14.

2. Results and Discussion

The frozen animals were cut into pieces and extracted exhaustively with acetone. Then an Et₂O-soluble portion of the acetone extract was repeatedly chromatographed over silica gel, Sephadex LH-20, and RP-HPLC to yield six new compounds 1, 3, 5–8, and four known analogs 2, 4, 9, and 10 (Figure 1). The known compounds were readily identified as sarcophyloide D (2) [42], sarcophytonolide H (4) [43], sarcophytrol O (9) [44], sinulaflexiolide I (10) [45], respectively, based on the comparison of their NMR spectral and specific optical data with those reported in the literature. In our previous work [43],

the absolute configuration of sarcophytonolide H (**4**) was established by the modified Mosher's method. In the present study, its crystals were obtained, which were suitable for X-ray diffraction experiment with Cu K α ($\lambda = 1.54178 \text{ \AA}$) radiation. The X-ray diffraction analysis allowed the assignment of the absolute configuration of **4** as 1*R*,2*R*,6*R*,14*S* (Fleck parameter: -0.03 (9)) (Figure 2, Table S2, CCDC 2205721), which was consistent with our previous study.

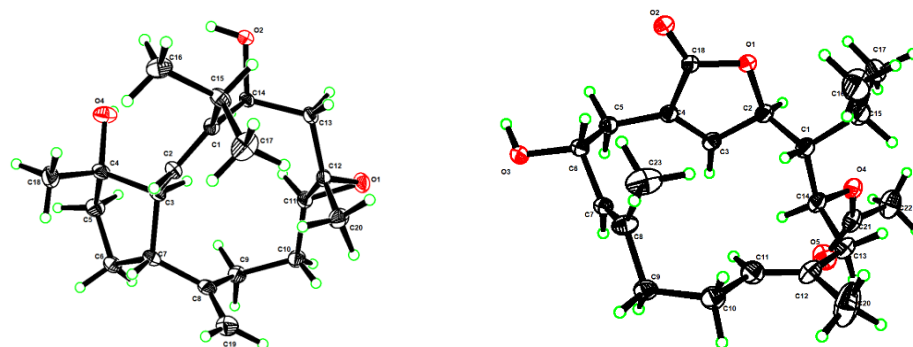


Figure 2. Perspective ORTEP drawing of the X-ray structures of compounds **1** (left) and **4** (right) (displacement ellipsoids are drawn at the 50% probability level).

Sartrocheliol A (**1**) was obtained as optically active colorless crystals. Its molecular formula $C_{20}H_{32}O_3$ was deduced from the protonated molecule peak at m/z 343.2243 ($[M + Na]^+$, calcd. for $C_{20}H_{32}O_3Na$, 343.2244) in the HRESIMS spectrum, implying five degrees of unsaturation. The IR spectrum indicated the presence of hydroxyl (ν_{max} 3441 cm^{-1}) and olefinic (ν_{max} $1660, 910 \text{ cm}^{-1}$) groups. The 1H and ^{13}C NMR spectra displayed the signals of a trisubstituted double bond (δ_H 5.14 (1H, d, $J = 12.6 \text{ Hz}$, H-2), δ_C 149.90 (qC, C-1), 125.85 (CH, C-2)), a terminal double bond (δ_H 4.88 (1H, s, H-19a), 4.69 (1H, s, H-19b), δ_C 148.54 (qC, C-8), 112.26 (CH $_2$, C-19)), an epoxide (δ_H 2.89 (1H, dd, $J = 10.6, 2.9 \text{ Hz}$, H-11), δ_C 62.28 (CH, C-11), 59.06 (qC, C-12)), an oxygenated methine (δ_H 4.88 (1H, dd, $J = 11.2, 5.1 \text{ Hz}$, H-14), δ_C 69.34 (CH, C-14)), and an oxygenated carbon (δ_C 81.64 (C, C-4)) (Tables 1 and 2). As revealed by the 1H and ^{13}C NMR data, there were two double bonds and one epoxide, accounting for three degrees of unsaturation. The remaining two degrees of unsaturation were due to the presence of two rings in the molecule. Considering the co-isolated secondary metabolite sarcophylolide D (**2**) [42], compound **1** was likely a capnosane-type diterpene. Indeed, the NMR data of **1** was almost identical to those of **2**, except for the chemical shift of C-11 (δ_C 62.28 for **1** vs. δ_C 59.54 for **2**). The interpretation of 1H - 1H COSY and HMBC spectra (Figure 3) indicated they shared the same gross structure. Analysis of the NOESY spectrum (Figure S6) revealed that there was lack of correlation between H-11 (δ_H 2.89) and H $_3$ -20 (δ_H 1.12), which revealed the *trans*-orientation of H-11 and H $_3$ -20 in **1**, the orientation of which was different from that of the isolate **2**. In order to check the proposed structure as well as establish the absolute configuration of **1**, a suitable single crystal was obtained in MeOH after many attempts. A successful performance of X-ray crystallography study using Cu K α ($\lambda = 1.54178 \text{ \AA}$) radiation firmly confirmed the structure of **1** and determined its absolute configuration ambiguously as 3*S*,4*S*,7*R*,11*S*,12*S*,14*S* (Fleck parameter: 0.05 (6)) (Figure 2, Table S1, CCDC 2196207). Hereto, the structure of **1** was established, as shown in Figure 1.

Sartrocheliol B (**3**) was isolated as optically active colorless oil. Its molecular formula $C_{22}H_{34}O_5$ was established by the HRESIMS protonated molecule peak at m/z 379.2482 ($[M + H]^+$, calcd. for $C_{22}H_{35}O_5$, 379.2479), which was indicative of six degrees of unsaturation. The IR spectrum of **3** suggested the presence of lactone (ν_{max} 1759 cm^{-1}), ester (ν_{max} 1736 cm^{-1}) and hydroxyl (ν_{max} 3442 cm^{-1}) groups, while a strong UV absorption at λ_{max} 231 nm ($\log \epsilon$ 3.83) suggested the presence of α,β -unsaturated γ -lactone group [43]. According to the 1H and ^{13}C NMR data of **3** (Tables 1 and 2), five degrees of unsaturation were attributed to one α,β -unsaturated γ -lactone group (δ_H 4.95 (1H, d, $J = 10.7 \text{ Hz}$, H-2),

7.44 (1H, t, $J = 1.8$ Hz, H-3), δ_C 81.19 (CH, C-2), 151.06 (CH, C-3), 131.39 (qC, C-4), 172.97 (qC, C-18)), one trisubstituted double bond (δ_H 5.05 (1H, t, $J = 7.7$ Hz, H-11), δ_C 129.20 (CH, C-11), 130.80 (qC, C-12)) and one acetyl group (δ_H 2.09 (3H, s), δ_C 21.35 (CH₃), 171.13 (qC)). The remaining one degree of unsaturation implied the monocyclic nature of this molecule. Considering the co-isolated cembranoids **4**, **9** and **10**, metabolite **3** was likely a cembrane-type diterpene. Through detailed literature reviews on diterpenes from the genus *Sarcophyton*, the above-mentioned structural features were reminiscent of previously reported sarcophytonolide H (**11**) [43], a cembrane from South China Sea soft coral *Sarcophyton latum*. Our interpretation of the 2D NMR spectra (Figure 3) suggested they differed by the lack of the double bond Δ^7 , which was supported by the significantly up-field shifted chemical shifts of C-7 and C-8 ($\Delta\delta_C$ ca. 80 and 110 ppm, respectively). Similar patterns of NOE correlations in the NOESY spectra of **3** and **11**, especially for the key NOE cross-peaks of H-2 (δ_H 4.95)/H-14 (δ_H 5.02), H-2/H₃-16 (δ_H 1.11), H-3 (δ_H 7.44)/H-5 (δ_H 2.45), and H-11 (δ_H 5.05)/H-13 (δ_H 2.20), indicated they shared the same configurations for the olefinic bonds Δ^3 and Δ^{11} and the chiral centers C-1, C-2, and C-14 (Figure 4). The clear NOE correlation of H-6 (δ_H 4.22)/H₃-19 (δ_H 0.77) suggested that H-6 and H₃-19 possessed the same orientation. Due to the lack of NOE correlations between the two sets: a. H-6 and H₃-19 and b. H-1, H-2 and H-14, the absolute configurations of these chiral centers corresponding to the above-mentioned two sets of protons were determined by the modified Mosher's method and CD spectrum, respectively. Treatment of **3** with (*R*)- and (*S*)- α -methoxy- α -trifluoromethylphenyl acetyl chlorides (MTPA-Cl) in dry pyridine successfully afforded the (*S*)- and (*R*)-MTPA ester derivatives **3s** and **3r**, respectively. The distribution pattern of observed $\Delta\delta_{H(S-R)}$ values (Figure 5) established the absolute configuration *S* for C-6 in **3**. Considering the correlation between H-6 and H₃-19, the absolute configuration of C-8 could be determined as *S*. It might be worth pointing out that the absolute configuration of sarcophytonolide H (**4**) had already been ambiguously confirmed as 1*R*,2*R*,6*R*,14*S* by the single crystal X-ray diffraction experiment in this study (Figure 2). The CD spectrum of **3** displayed the Cotton effect resembling that of co-isolated **4** (Figure 6), suggesting they shared the same absolute configuration *R* for the chiral carbon C-2 of the chromophore α,β -unsaturated γ -lactone. With the relationships of H-1, H-2, and H-14 in hand, the absolute configurations of C-1 and C-14 could be assigned as *R* and *S*, respectively. Consequently, the absolute configuration of **3** could be established as 1*R*,2*R*,6*S*,8*S*,14*S*.

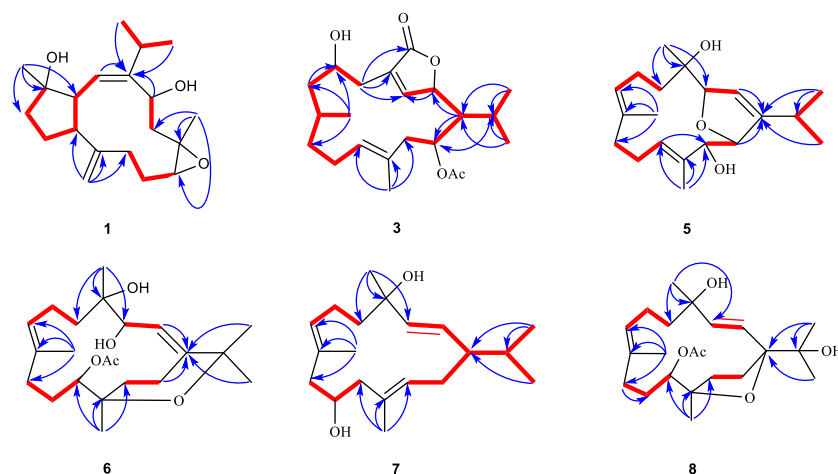
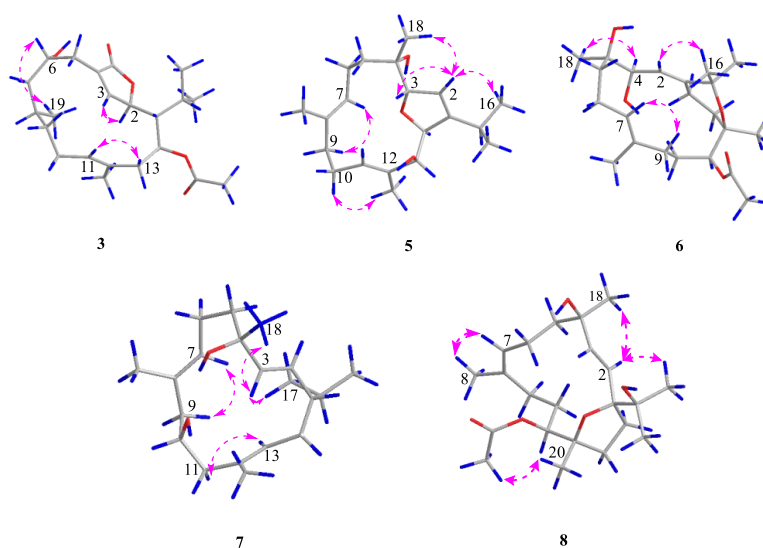
Table 1. ¹H NMR spectroscopic data of sartocheiliols A–E (**1**, **3**, **5**–**8**) in CDCl₃.

No.	1 ^a	3 ^b	5 ^b	6 ^b	7 ^b	8 ^a
1		1.55 (d, 10.7)			1.54 (br s)	
2	5.14 (d, 10.6)	4.95 (d, 10.7)	5.51 (d, 1.4)	5.42 (m)	5.51 (dd, 15.6, 9.6)	5.56 (d, 15.6)
3	2.84 (t, 10.6)	7.44 (t, 1.8)	4.66 (dq, 5.5, 1.4)	4.40 (br s)	5.63 (d, 15.6)	6.13 (d, 15.9)
4						
5	1.84 (m)	2.75 (dt, 13.2, 1.2)	1.83 (m)	1.94 (m)	1.89 (ddd, 13.4, 8.6, 1.9)	1.87 (m)
	1.78 (m)	2.45 (dd, 13.3, 10.5)	1.53 (m)	1.76 (m)	1.58 (m)	1.69 (m)
6	1.66 (m)	4.22 (t, 9.8)	2.34 (m)	2.06 (m)	2.24 (m)	2.64 (m)
			1.92 (m)			
7	2.48 (t, 7.1)	1.63 (m)	5.22 (m)	5.24 (t, 6.3)	5.11 (d, 7.8)	5.43 (dd, 10.6, 4.0)
		1.35 (m)				
8		1.29 (m)				
9	2.33 (m)	1.36 (m)	2.10 (m)	1.96 (m)	2.25 (m)	2.00 (m)
	2.00 (t, 13.5)	1.26 (m)		1.67 (m)	2.12 (m)	
10	2.21 (m)	2.08 (m)	2.26 (m)	1.86 (m)	4.07 (d, 10.9)	1.90 (m)
	1.46 (m)		2.11 (m)	1.43 (m)		1.55 (m)
11	2.89 (dd, 10.6, 2.9)	5.05 (t, 7.7)	5.32 (m)	5.04 (d, 10.3)	2.09 (m)	5.08 (d, 9.4)
12						
13	2.25 (m)	2.26 (dd, 13.5, 3.0)	4.29 (t, 4.3)	1.94 (m)	5.24 (t, 7.7)	1.78 (m)
	1.65 (m)	2.20 (dd, 13.5, 10.9)		1.61 (m)		1.59 (m)
14	4.88 (dd, 11.2, 5.1)	5.02 (ddd, 10.8, 4.2, 1.1)	4.84 (td, 5.0, 1.6)	3.04 (m)	2.07 (m)	2.33 (td, 11.8, 7.4)
				2.38 (m)		1.68 (m)
15	2.48 (m)	2.22 (m)	2.65 (m)		1.70 (m)	
16	1.12 (d, 6.5)	1.11 (d, 6.6)	1.16 (d, 6.8)	1.37 (s)	0.96 (d, 6.6)	1.11 (s)
17	1.16 (d, 6.5)	1.12 (d, 6.6)	1.08 (d, 6.9)	1.30 (s)	0.84 (d, 6.7)	1.13 (s)
18	1.16 (s)		1.00 (s)	1.20 (s)	1.30 (s)	1.35 (s)
19	4.88 (s)	0.77 (d, 6.0)	1.56 (s)	1.56 (s)	1.54 (s)	1.71 (s)
	4.69 (s)					
20	1.12 (s)	1.67 (s)	1.56 (s)	1.10 (s)	1.57 (m)	1.17 (s)
OAc		2.09 (s)		2.08 (s)		2.05 (s)

^a 500 MHz. ^b 600 MHz.

Table 2. ^{13}C NMR spectroscopic data (125 MHz, CDCl_3) of sartracheliols A–E (1, 3, 5–8).

No.	1	3	5	6	7	8
1	149.90, qC	49.67, CH	150.34, qC	146.95, qC	51.96, CH	91.52, qC
2	125.85, CH	81.19, CH	121.20, CH	121.34, CH	122.10, CH	129.84, CH
3	51.08, CH	151.06, CH	87.63, CH	73.16, CH	141.04, CH	137.41, CH
4	81.64, qC	131.39, qC	74.93, qC	75.86, qC	74.20, qC	72.47, qC
5	41.04, CH_2	37.42, CH_2	39.37, CH_2	39.18, CH_2	44.21, CH_2	41.64, CH_2
6	25.90, CH_2	66.40, CH	22.57, CH_2	21.75, CH_2	23.66, CH_2	22.90, CH_2
7	54.09, CH	47.19, CH_2	128.74, CH	127.40, CH	127.31, CH	130.06, CH
8	148.54, qC	28.31, CH	133.16, qC	134.03, qC	130.05, qC	132.11, qC
9	24.65, CH_2	37.25, CH_2	39.64, CH_2	33.90, CH_2	46.88, CH_2	34.86, CH_2
10	28.07, CH_2	24.31, CH_2	25.00, CH_2	25.03, CH_2	68.82, CH	27.37, CH_2
11	62.28, CH	129.20, CH	130.08, CH	72.70, CH	38.96, CH_2	77.36, CH
12	59.06, qC	130.80, qC	132.19, qC	74.15, qC	132.94, qC	84.58, qC
13	45.46, CH_2	41.43, CH_2	79.67, CH	29.33, CH_2	128.47, CH	35.80, CH_2
14	69.34, CH	73.92, CH	86.05, CH	20.95, CH_2	23.68, CH_2	30.76, CH_2
15	27.09, CH	25.81, CH	27.43, CH	74.60, qC	29.13, CH	72.84, qC
16	21.23, CH_3	24.93, CH_3	21.11, CH_3	30.42, CH_3	21.15, CH_3	26.01, CH_3
17	23.55, CH_3	18.74, CH_3	22.57, CH_3	28.85, CH_3	21.85, CH_3	24.62, CH_3
18	27.70, CH_3	172.97, qC	23.36, CH_3	21.72, CH_3	29.17, CH_3	29.00, CH_3
19	112.26, CH_2	18.25, CH_3	15.84, CH_3	17.41, CH_3	15.52, CH_3	16.33, CH_3
20	23.05, CH_3	18.47, CH_3	12.89, CH_3	23.63, CH_3	15.09, CH_3	20.69, CH_3
OAc		171.13, qC		170.47, qC		170.17, qC
		21.35, CH_3		21.75, CH_3		21.42, CH_3

**Figure 3.** The selected key ^1H – ^1H COSY (red lines) and HMBC (blue arrows, from ^1H to ^{13}C) correlations of compounds 1, 3, 5–8.**Figure 4.** The selected key NOESY (pink dashed lines, from ^1H to ^1H) correlations of compounds 3, 5–8.

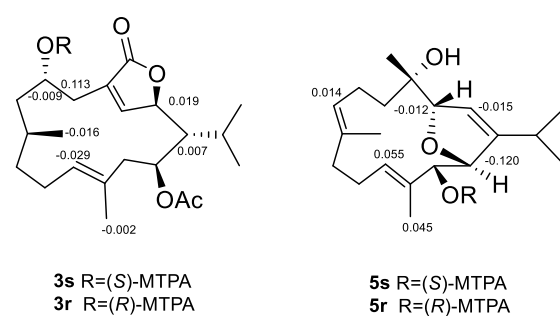


Figure 5. $\Delta\delta$ values ($\delta_S - \delta_R$) (ppm) for (S)- and (R)-MTPA esters of 3 and 5.

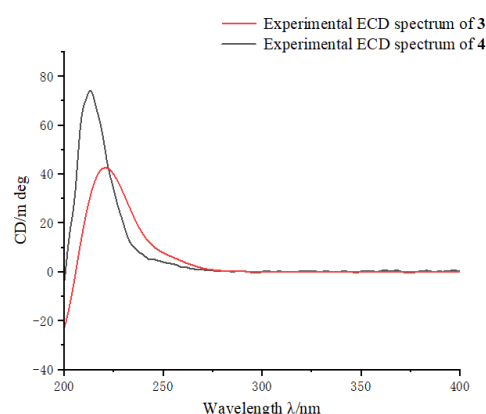


Figure 6. ECD curves of compounds 3 (up) and 4 (down).

The protonated molecule peak at m/z 343.2237 ($[M + Na]^+$, calcd. for $C_{20}H_{32}O_3Na$, 343.2244) displayed in the HRESIMS spectrum of sartrocheliol C (5) revealed that compound 5 had the molecular formula $C_{20}H_{32}O_3$, demonstrating the presence of an additional oxygen atom with respect to that of a dihydrofuran cembranoid 12 [46]. The IR spectrum of 5 showed the presence of olefinic (ν_{max} 3726 cm^{-1}) and hydroxyl (ν_{max} 3441 cm^{-1}) groups. A careful analysis of its NMR spectra revealed that the NMR spectroscopic features of 5 (Tables 1 and 2) highly resembled those of 12. In fact, the main difference between compounds 5 and 12 was that the CH_2 -13 in 12 was hydroxylated in 5. The presence of a hydroxyl group at C-13 was supported by the dramatically down-field shifted carbon chemical shift ($\Delta\delta_C$ 56 ppm), and further confirmed by the diagnostic HMBC correlations of from H-11 (δ_H 5.32) to C-13 (δ_C 79.67) and from H₃-20 (δ_H 1.56) to C-13 (Figure 3). The cross-peak of H₃-18 (δ_H 1.00)/H-2 (δ_H 5.51) observed in the NOESY spectrum of 5 (Figure 4) together with the small coupling constant (1.4 Hz) between H-2 and H-3 (δ_H 4.66) suggested the same orientation of H₃-18 and H-3. Moreover, the coupling constant (4.6 Hz) between H-13 (δ_H 4.29) and H-14 (δ_H 4.84) indicated these two protons were *cis*-orientated. Whereas the lack of the NOE correlation between H-3 and H-14 revealed the *trans*-orientation of these two protons of the 2,5-dihydrofuran ring. Thus, the relative configuration of 5 could be assigned as $3R^*,4R^*,13S^*,14S^*$ based on the extensive analysis of the NOESY spectrum. Meanwhile, the relative configuration of 5 could also be elucidated via QM-NMR protocol by using the DP4+ method, which has become one of the most popular and reliable methods to find the most likely structure from a set of putative candidates [34,47]. Four possible isomers ($2R^*,3R^*,13R^*,14S^*$)-5a, ($2R^*,3R^*,13S^*,14S^*$)-5b, ($2R^*,3S^*,13R^*,14S^*$)-5c and ($2R^*,3S^*,13S^*,14R^*$)-5d (Table S3) were subjected to QM-NMR calculations. As a result, the experimental NMR data of compound 5 gave the best match for 5b, with 100% probability (Figure 7, Table S4). Herein, the assigned relative configuration $3R^*,4R^*,13S^*,14S^*$ was consistent with the observations deduced from the NOESY spectrum. As there was a secondary hydroxyl group at C-13, the modified Mosher's method was applied. The resulting distribution pattern of observed $\Delta\delta_{H(S-R)}$ values (Figure 5) established the absolute

configuration *R* for C-13 in **5**. Subsequently, the absolute configuration of **5** could be assigned as *3S,4S,13R,14R*.

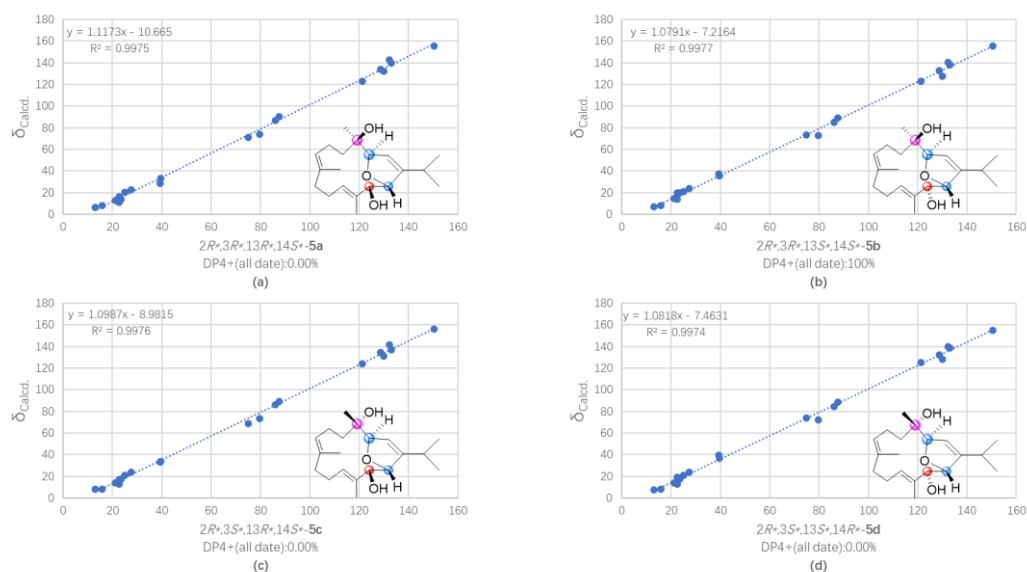


Figure 7. Regression analysis of experimental vs. calculated ^{13}C NMR chemical shifts of (a) ($2R^*,3R^*,13R^*,14S^*$)-**5a**, (b) ($2R^*,3R^*,13S^*,14S^*$)-**5b**, (c) ($2R^*,3S^*,13R^*,14S^*$)-**5c**, and (d) ($2R^*,3S^*,13S^*,14R^*$)-**5d** at the PCM/mPW1PW91/6-31 + G** level, using the DP4+ method.

The HRESIMS spectrum of sartrocheliol D (**6**) displayed a protonated molecule peak at m/z 403.2459 ($[\text{M} + \text{Na}]^+$, calcd. for $\text{C}_{22}\text{H}_{36}\text{O}_5\text{Na}$, 403.2455), suggesting that **6** possessed the molecular formula $\text{C}_{22}\text{H}_{36}\text{O}_5$. Thus, five degrees of unsaturation were determined for **6**. The NMR data (Tables 1 and 2) revealed the presence of two trisubstituted double bonds (δ_{H} 5.42 (1H, m, H-2), δ_{C} 146.95 (qC, C-1), 121.34 (CH, C-2); δ_{H} 5.24 (1H, t, $J = 6.3$ Hz, H-7), δ_{C} 127.40 (CH, C-7), 134.03 (qC, C-8)), one acetyl group (δ_{H} 2.08 (3H, s), δ_{C} 21.75 (CH₃), 170.47 (qC)), two oxygenated methines (δ_{H} 4.40 (1H, br s, H-3), 5.04 (1H, d, $J = 10.3$ Hz, H-11), δ_{C} 72.70 (CH, C-11), 73.16 (CH, C-3)), and three oxygenated quaternary carbons (δ_{C} 75.86 (qC, C-4), 74.15 (qC, C-12), 74.60 (qC, C-15)), which accounted for three degrees of unsaturation. The remaining two degrees of unsaturation strongly indicated one macrocyclic carbon skeleton fused with an oxacycle. Careful analysis of the 2D NMR spectrum (Figure 3) of **6** revealed this compound had almost the same gross bicyclic framework of sarcophytrol R (**13**) [44] except the hydroxyl group at C-11 in **13** was acetylated in **6**. Due to the acetylation, the chemical shifts of H-11 and C-11 shifted down-field ($\Delta\delta_{\text{H}}$ 1.5 ppm, $\Delta\delta_{\text{C}}$ 3.2 ppm, respectively). It might be worth pointing out that the lists of ^1H and ^{13}C NMR data of sarcophytrols R and S in the reference [44] were exchanged inadvertently by the authors. The high similarity of the ^1H and ^{13}C NMR data as well as similar patterns of NOE correlations of compounds **6** and **13** suggested they shared the same relative configuration $3S^*,4R^*,11S^*,12R^*$. With the relative configuration in hand, we tried to use the Mosher's method to establish the absolute configuration of this compound. However, to our disappointment, the left compound after bioassay was degraded although kept in a fridge.

Sartrocheliol E (**7**) was isolated as colorless oil, and its molecular formula was assigned as $\text{C}_{20}\text{H}_{34}\text{O}_2$ by protonated molecule peak at m/z 329.2448 ($[\text{M} + \text{Na}]^+$, calcd. for $\text{C}_{20}\text{H}_{34}\text{O}_2\text{Na}$, 329.2451) in the HRESIMS spectrum. Its ^{13}C NMR data (Table 2), in combination with the DEPT and HSQC spectra, allowed the identification of 20 carbon resonances, involving six olefinic carbons (δ_{C} 141.04, 132.94, 130.05, 128.47, 127.31, 122.10), two oxygenated carbons (δ_{C} 74.20, 68.82), and five methyl carbons (δ_{C} 29.17, 21.85, 21.15, 15.52, 15.09). The presence of six olefinic carbons was attributed to three double bonds, which accounted for three degrees of unsaturation, indicating that **7** had a monocyclic carbon

framework. In fact, the NMR spectroscopic characters of **7** were reminiscent of those of cembreniol (**14**) [48]. Careful comparison of their NMR data disclosed their structures differed at the position of the secondary hydroxyl substituent. The secondary hydroxyl group substituted at C-10 in **7** was supported by the consecutive proton system extending from H₂-9 to H₂-11 through H-10 in the ¹H–¹H COSY spectrum (Figure 3). Due to the lack of the evidence regarding the orientations of H-10 and H₃-18, it was hard to figure out the relative configurations of C-4 and C-10. In order to solve this problem, the QM-NMR method was applied (Table S5). By means of this approach, the experimentally observed NMR data for compound **7** gave the best match with the 1*S**,4*R**,10*S** isomer (>90% probability) (Figure 8, Table S6). Thus, the relative configuration of compound **7** was determined as 1*S**,4*R**,10*S**. Unfortunately, the application of Mosher's reaction failed, probably due to the insufficient amounts left after an array of bioassays.

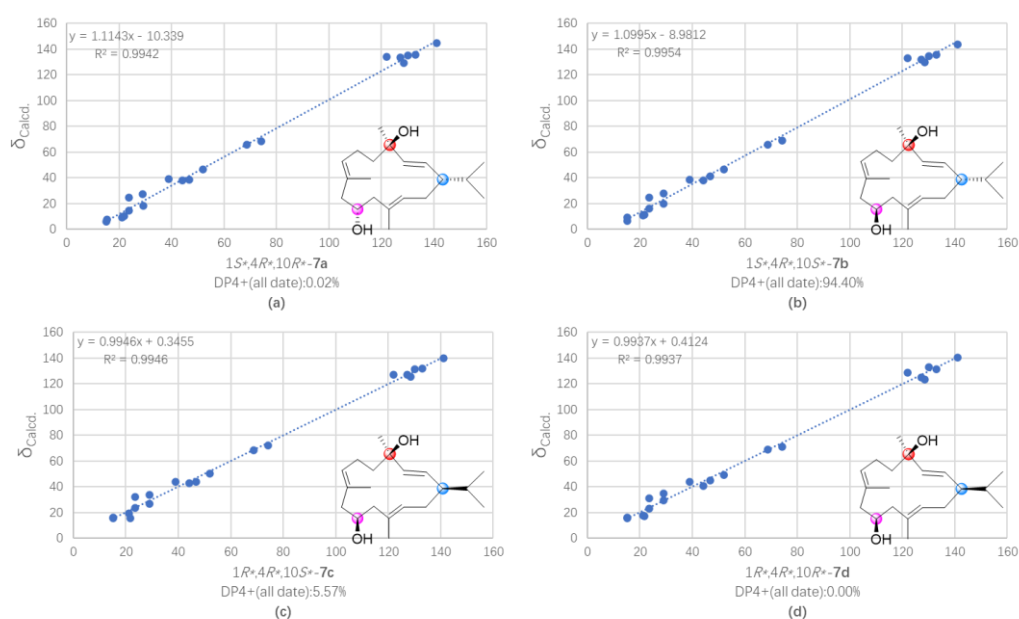


Figure 8. Regression analysis of experimental vs. calculated ¹³C NMR chemical shifts of (a) (1*S**,4*R**,10*R**)-7a, (b) (1*S**,4*R**,10*S**)-7b, (c) (1*R**,4*R**,10*S**)-7c, and (d) (1*R**,4*R**,10*R**)-7d at the PCM/mPW1PW91/6-31 + G** level, using the DP4+ method.

The protonated molecule peak at *m/z* 403.2446 ([M + Na]⁺, calcd. for C₂₂H₃₆O₅Na, 403.2455) in the HRESIMS spectrum of sartrocheliol F (**8**) suggested compound **8** and co-isolate **9** [44] had the same molecular formula C₂₂H₃₆O₅. Moreover, the NMR data of **8** (Tables 1 and 2) highly resembled those of **9**, implying that they shared the same gross structure. The distinct difference was found as the chemical shift of C-4, which was δ_C 72.47 ppm in **8** whereas δ_C 74.49 ppm in **9**, disclosing the reverse configuration of the hydroxyl group at C-4. This reversion was further deduced from the NOE interactions between H₃-18 and H-2 and between H-2 and H₃-16 (Figure 4). As the absolute configuration of the deacetylation derivative of **9** was determined as 1*S*,4*S*,11*S*,12*R* by the Mosher's method [44], the absolute configuration of **8** was consequently established as 1*S*,4*R*,11*S*,12*R*.

Although chemical investigations of the soft coral *S. trocheliophorum* have been well documented in the literature, the present study of this species collected from Ximao Island provided further intriguing results. In the current study, six new cembranoids diterpenoids, sartrocheliols A–E (**1**, **3**, **5**–**8**), along with four known related ones (**2**, **4**, **9**, and **10**) were obtained. Among them, compound **1** was a capnosane diterpene, while others were cembrane diterpenes. They displayed diverse structural features not only at the distinctly different carbon frameworks but also at the various types of heterocycles, including the epoxide, γ-lactone, furan, and pyran rings. Compared with the previous research of the Ximao Island specimen [41], the major difference was the discovery of a capnosane

diterpene in this study. This observation further indicated the possible impact of temporal variations on the different metabolic processes for the title soft corals.

The anti-tumor effects of all the ten secondary metabolites were evaluated against a list of tumor cells including A549 (human lung cancer cell), H1975 (human lung adenocarcinoma cell), MDA-MB-231 (human breast cancer cell) and H1299 (human non-small cell lung cancer cell). The results showed compound **4** displayed moderate cytotoxic activities against these four cells with the IC_{50} values of 47.9, 26.3, 44.7, 33.1 μ M, respectively, while **6** only showed moderate cytotoxicity against H1975 (IC_{50} = 40.4 μ M). Further, we also conducted molecular interaction experiments on all the compounds, looking for compounds that have the potential to bind to BRD4 and ROR1 anti-tumor targets, respectively. Unfortunately, we did not obtain satisfactory results. In addition, these compounds were tested for their antibacterial activities against a vast array of bacteria including the human pathogens *Staphylococcus aureus* ATCC27154, *Enterococcus faecium*, *Escherichia coli* ATCC25922, *Enterobacter cloacae* ZR042, *Enterobacter hormaechei* 2R043, *Pseudomonas aeruginosa* ATCC10145, methicillin-resistant *Staphylococcus aureus* (MRSA), and *Candida albicans* ATCC76485 and the marine strains *Streptococcus parauberis* KSP28, *Streptococcus parauberis* SPOF3K, *Lactococcus garvieae* MP5245, *Aeromonas salmonicida* AS42, *Phyobacterium damsela* FP2244, *Pseudomonas fulva* ZXM181, *Photobacterium halotolerans* LMG22194T. To our disappointment, all of them were judged as inactive. Other bioassays such as neuroprotective and anti-inflammatory are currently on the way.

3. Materials and Methods

3.1. Subsection

Melting points were measured on an X-4 digital micromelting point apparatus. The X-ray measurements were made on a Bruker D8 Venture X-ray diffractometer with Cu $K\alpha$ radiation (Bruker Biospin AG, Fällanden, Germany). IR spectra were recorded on a Nicolet iS50 spectrometer (Thermo Fisher Scientific, Madison, WI, USA). Optical rotations were measured on a PerkinElmer 241MC polarimeter (PerkinElmer, Fremont, CA, USA). CD & UV spectra were measured on a JASCO J-810 instrument (JASCO Corporation, Tokyo, Japan). 1H and ^{13}C NMR spectra were acquired on a Bruker AVANCE III 400 and 600 MHz spectrometer (Bruker Biospin AG, Fällanden, Germany). Chemical shifts were reported with the residual $CHCl_3$ (δ_H 7.26; δ_C 77.16) as the internal standard for 1H and ^{13}C NMR spectra. The LREIMS and HREIMS data were recorded on a Finnigan-MAT-95 mass spectrometer (Finnigan-MAT, San Jose, CA, USA). HRESIMS spectra were recorded on Agilent G6250 Q-TOF (Agilent, Santa Clara, CA, USA). Commercial silica gel (Qingdao Haiyang Chemical Co., Ltd., Qingdao, China, 200–300 mesh, 300–400 mesh) was used for column chromatography, and precoated silica gel GF254 plates (Sinopharm Chemical Reagent Co., Shanghai, China) were used for analytical TLC. Sephadex LH-20 (Pharmacia, Piscataway, NJ, USA) was also used for column chromatography. Reversed-phase (RP) HPLC was performed on an Agilent 1260 series liquid chromatography equipped with a DAD G1315D detector at 210 nm (Agilent, Santa Clara, CA, USA). An Agilent semi-preparative XDB-C18 column (5 μ m, 250 \times 9.4 mm) was employed for the purification. All solvents used for column chromatography and HPLC were of analytical grade (Shanghai Chemical Reagents Co., Ltd., Shanghai, China) and chromatographic grade (Dikma Technologies Inc., Foothill Ranch, CA, USA), respectively.

3.2. Animal Material

The soft coral *Sarcophyton trocheliophorum* was collected by scuba at a depth of 15 m in May 2018 in Ximao Island, Hainan Province, China. The animal material was identified by Prof. Xiu-Bao Li from Hainan University. A voucher specimen (No. 18XD-19) is available for inspection at the Shanghai Institute of Materia Medica, CAS.

3.3. Extraction and Isolation

The frozen animals (551 g, dry weight) were cut into pieces and extracted exhaustively with acetone at room temperature (3×3 L, 30 min in ultrasonic bath). The organic extract was evaporated to give a brown residue (80 g), which was partitioned between Et₂O and H₂O. The Et₂O solution was concentrated under reduced pressure to give a dark brown residue (55.3 g), which was fractionated by gradient silica gel (200–300 mesh) column chromatography (0 → 100% Et₂O in petroleum ether (PE)), yielding seven fractions (A–G). Fractions E and F were subjected to a column of Sephadex LH-20 eluted with CH₂Cl₂ and PE/CH₂Cl₂/MeOH (2:1:1) to remove the fatty acids and give ten subfractions (EA–EF and FA–FF), respectively. The subfraction EE was purified by semi-preparative HPLC (60% → 100% MeCN in 20 min, 2.5 mL/min), yielding compounds **5** (3.6 mg; *t*_R 10.0 min) and **10** (1.5 mg; *t*_R 12.0 min). FCA-FCC was got from subfraction FC by silica gel column chromatography (300–400 mesh, PE/Et₂O (100:1 → 70:1)). The subfraction FCA afforded compounds **2** (1.0 mg; *t*_R 7.1 min), **6** (0.9 mg; *t*_R 17.0 min), **8** (0.9 mg; *t*_R 18.9 min) and **9** (2.0 mg; *t*_R 12.0 min) through semi-preparative HPLC (70% MeCN, 2.5 mL/min). While subfraction FCB gave compounds **1** (1.3 mg; *t*_R 7.0 min) and **7** (1.6 mg; *t*_R 16.0 min), through semi-preparative HPLC (70% MeCN, 2.5 mL/min) as well. The subfraction FD afforded compounds **3** (3.2 mg; *t*_R 6.2 min) and **4** (8.0 mg; *t*_R 5.5 min) through semi-preparative HPLC (70% MeCN, 2.5 mL/min).

3.4. Spectroscopic Data of Compounds

Sartrocheliol A (**1**): colorless crystals; $[\alpha]_D^{20} +250.0$ (*c* 0.05, MeOH); IR (KBr) ν_{\max} : 3441, 2925, 1384 cm⁻¹; ¹H and ¹³C NMR data, see Tables 1 and 2; HRESIMS *m/z* 343.2243 [M + Na]⁺ (calcd. for C₂₀H₃₂NaO₃, 343.2244).

Sartrocheliol B (**3**): colorless oil; $[\alpha]_D^{20} +12.7$ (*c* 0.05, MeOH); UV (MeOH) λ_{\max} (log ϵ) 240 (3.23) nm; CD (MeOH) λ_{\max} ($\Delta\epsilon$) 240 (+4.06), 285 (−1.92) nm; IR (KBr) ν_{\max} : 3442, 2932, 1759, 1736, 1234, 1047, 1023 cm⁻¹; ¹H and ¹³C NMR data, see Tables 1 and 2; HRESIMS *m/z* 379.2479 [M + H]⁺ (calcd. for C₂₂H₃₄O₅, 379.2482).

Sartrocheliol C (**5**): colorless oil; $[\alpha]_D^{20} -12.7$ (*c* 0.1, MeOH); IR (KBr) ν_{\max} : 3726, 3624, 3441, 2960, 1384, 1087, 1032 cm⁻¹; ¹H and ¹³C NMR data, see Tables 1 and 2; HRESIMS *m/z* 343.2237 [M + Na]⁺ (calcd. for C₂₀H₃₂NaO₃, 343.2244).

Sartrocheliol D (**6**): colorless oil; $[\alpha]_D^{20} -20.0$ (*c* 0.05, MeOH); IR (KBr) ν_{\max} : 3443, 2927, 1384, 1038 cm⁻¹; ¹H and ¹³C NMR data, see Tables 1 and 2; HRESIMS *m/z* 403.2459 [M + Na]⁺ (calcd. for C₂₂H₃₆NaO₅, 403.2455).

Sartrocheliol E (**7**): colorless oil; $[\alpha]_D^{20} +120.0$ (*c* 0.01, MeOH); IR (KBr) ν_{\max} : 3446, 2922, 1384, 1142, 1044 cm⁻¹; ¹H and ¹³C NMR data, see Tables 1 and 2; HR-ESIMS *m/z* 329.2448 [M + Na]⁺ (calcd. for C₂₀H₃₄NaO, 329.2451).

Sartrocheliol F (**8**): colorless oil; $[\alpha]_D^{20} +40.0$ (*c* 0.05, MeOH); IR (KBr) ν_{\max} : 3442, 1384 cm⁻¹; ¹H and ¹³C NMR data, see Tables 1 and 2; HR-ESIMS *m/z* 403.2446 [M + Na]⁺ (calcd. for C₂₂H₃₆NaO₅, 403.2455).

3.5. X-ray Crystallographic Analysis for Compounds 1 and 4

The crystals of **1** and **4** were both recrystallized from methanol at 4 °C. X-ray analysis of **1** and **4** were carried out on a Bruker D8 Venture diffractometer with Cu K α radiation ($\lambda = 1.54178$ Å) at 170 K, respectively. The acquisition parameters for **1** and **4** are provided in the Supplementary Materials, and crystallographic data for compounds **1** and **4** (deposition no. CCDC 2,196,207 and CCDC 2205721) have been deposited at the Cambridge Crystallographic Data Center. Copies of the data can be obtained free of charge via www.ccdc.cam.ac.uk/conts/retrieving.html (accessed on 11 August 2022).

3.6. Esterification of Compounds 3 and 5 with MTPA Chlorides

Compounds **3** and **5** (2.0 mg each) were dissolved in dry pyridine (1.2 mL), divided them into two sets (0.6 mL each), then treated with (*R*)-(−)-2-methoxy-2-(trifluoromethyl) phenylacetyl chloride ((*R*)-(−)-MTPA-Cl) (10 μ L) and (*S*)-(+)-2-methoxy-2-(trifluoromethyl)

phenylacetyl chloride ((*S*)-(+)-MTPA-Cl) (10 μ L), respectively. After stirring overnight at room temperature, the solutions were evaporated in vacuo and the residues were purified by silica gel column chromatography (PE/Et₂O = 90:10) to obtain the *S*-MTPA ester **3r** (0.3 mg), *R*-MTPA ester **3s** (0.3 mg), *S*-MTPA ester **5r** (0.3 mg), and *R*-MTPA ester **5s** (0.3 mg), respectively. The obtained products were then subjected to the ¹H NMR experiment.

3.7. QM-NMR Calculation of Compounds **5** and **7**

Theoretical calculations of all theoretical stereoisomers were carried out to determine the relative configuration of **5** and **7**, based on the alignment of its ¹D NMR chemical shifts (¹³C NMR chemical shifts herein) and calculation-generated chemical shifts. Confab was used to search the conformational space of **5a–5d** and **7a–7d**. Conformational searches were carried out using the torsional sampling (MCMM) method and OPLS_2005 force field in the MacroModel 9.9.223 software applying an energy window of 21 kJ/mol. Conformers above 1% population were re-optimized with Gaussian 09 at the B3LYP/6-311G(d,p) level with IEFPCM (Polarizable Continuum Model using the Integral Equation Formalism variant) solvent model for acetonitrile. The Boltzmann populations of the conformers were obtained based on the potential energy provided by the OPLS_2005 force field, leading to 11, 9, 13 and 24 conformers for **5a–5d**; 11, 9, 13 and 24 conformers for **7a–7d** above 1% population for further re-optimization, respectively. The obtained conformers were subjected to optimization and frequency calculations on B3LYP/6-311G(d,p) level of theory. GIAO DFT ¹³C NMR calculations were calculated on mPW1PW91/6-31G* (CHCl₃) level of theory, and the calculated shielding tensors were Boltzmann averaged according to Gibbs free energy and then converted into chemical shifts following MSTD protocol. The experimental ¹³C NMR data of **5** and **7** were compared with the calculated NMR chemical shifts of **5a–5d** and **7a–7d** using the mean absolute error (MAE) values, maximum deviation (MD) values, correlation coefficient (R²), and DP4+ probability analysis. XYZ data for all conformations and detailed data for DP4+ analysis are provided in the Supplementary Materials.

3.8. Cytotoxic Bioassays

H1975, MDA-MB-231, A549, and H1299 cancer cell lines were purchased from the Procell Life Science & Technology Co., Ltd. Cells were cultured at 37 °C in a 5% CO₂ humidified incubator and maintained in high glucose Dulbecco's Modified Eagle Medium (DMEM, Nissui, Tokyo, Japan) containing 100 mg/mL streptomycin, 2.5 mg/L amphotericin B and 10% heat-inactivated fetal bovine serum (FBS). The cells were inoculated in 96-well culture plates for 12 h and then treated with different concentrations of compounds for 72 h. Water-soluble tetrazole (WST) reagent was added to each (10 μ L) well and cultured at 37 °C for 2 h to assess cell viability. The absorbance was read with a microplate reader at 450 nm. Adriamycin (DOX) was the positive control.

4. Conclusions

In summary, the present investigation of the soft coral *S. trocheliophorum* from Ximao Island provided intriguing results including six new cembranoids diterpenoids, sartrocheliols A–E (**1**, **3**, **5–8**), along with four known related ones (**2**, **4**, **9**, and **10**). This study not only extended the members of capnosane and cembrane diterpenes but also enriched the chemical diversity of the title species. In addition, a whole set of NMR computations, modified Mosher's method, and X-ray diffraction analysis were applied to assign the absolute configurations of compounds **1**, **3**, **4**, and **5**. However, the absolute configurations of other new metabolites remain undefined. To achieve it, a collection of the biological materials and accumulation of these new compounds should be conducted in future, which could supply sufficient amounts of metabolites for either the subsequent chemical transformations or recrystallization experiments. Anti-tumor and antibacterial bioassays were carried out. Among these secondary metabolites, compound **4** displayed moderate cytotoxicity against A549, H1975, MDA-MB-231, and H1299 cells (IC₅₀ = 47.9, 26.3, 44.7, 33.1 μ M, respectively), while **6** only exhibited moderate cytotoxicity against H1975 (IC₅₀ = 40.4 μ M). However,

none of them were active in the antibacterial bioassay. Moreover, the bioactivities of these compounds such as anti-virus, will be evaluated in future.

Supplementary Materials: The following supporting information can be downloaded at: <https://www.mdpi.com/article/10.3390/md21020069/s1>, Figures S1–S48: NMR, HRESIMS and IR data of compounds **1**, **3**, **5–8**; Figures S49 and S50: Regression analysis of experimental vs. calculated ¹³C NMR chemical shifts of different isomers of compounds **5** and **7** at the PCM/mPW1PW91/6-31 + G** level using DP4+ method; Tables S1 and S2: X-ray crystallographic data for compounds **1** and **4**; Tables S3 and S5: Cartesian coordinates of all conformers of isomers **5a–5b** and **7a–7b** used after optimization at the B3LYP/6-311G (d,p) level of theory as required for DP4+ analysis; Tables S4 and S6: DP4+ results obtained using experimental data of compounds **5 versus** isomers **5a–5b** and **7 versus** isomers **7a–7b**.

Author Contributions: Conceptualization, L.-F.L., F.Y. and Y.-W.G.; methodology, L.-F.L., F.Y. and Y.-W.G.; validation, Y.-T.S., M.-Z.S., H.L. and J.-G.C.; formal analysis, Y.-T.S. and D.-D.Y.; investigation, Y.-T.S. and D.-D.Y.; data curation, Y.-T.S. and D.-D.Y.; writing—original draft preparation, Y.-T.S.; writing—review and editing, L.-F.L. and Y.-W.G.; supervision, Y.-W.G.; project administration, Y.-W.G.; funding acquisition, L.-F.L. and Y.-W.G. All authors have read and agreed to the published version of the manuscript.

Funding: This research work was financially supported by the National Natural Science Foundation of China (NSFC) (Nos. 81991521 and 41876194), the National Key Research and Development Program of China (No. 2022YFC2804100), and the SKLDR/SIMM Project (No. SIMM2103ZZ-06).

Institutional Review Board Statement: Not applicable.

Informed Consent Statement: Not applicable.

Data Availability Statement: The data presented in this study are available on request from the corresponding author.

Acknowledgments: We thank X.-B. Li from Hainan University for the taxonomic identification of the soft coral material.

Conflicts of Interest: The authors declare no conflict of interest.

References

1. Anjaneyulu, A.S.R.; Rao, G.V. Chemical constituents of the soft coral species of *Sarcophyton* genus: A review. *J. Indian Chem. Soc.* **1997**, *74*, 272–278.
2. Liang, L.-F.; Guo, Y.-W. Terpenes from the soft corals of the genus *Sarcophyton*: Chemistry and biological activities. *Chem. Biodivers.* **2013**, *10*, 2161–2196. [[CrossRef](#)]
3. Zubair, M.S.; Al-Footy, K.O.; Ayyad, S.-E.N.; Al-Lihaibi, S.S.; Alarif, W.M. A review of steroids from *Sarcophyton* species. *Nat. Prod. Res.* **2016**, *30*, 869–879. [[CrossRef](#)]
4. Elkhawas, Y.A.; Elissawy, A.M.; Elnaggar, M.S.; Mostafa, N.M.; Al-Sayed, E.; Bishr, M.M.; Singab, A.N.B.; Salama, O.M. Chemical diversity in species belonging to soft coral genus *Sarcophyton* and its impact on biological activity: A review. *Mar. Drugs* **2020**, *18*, 41. [[CrossRef](#)]
5. Wang, Z.; Tang, H.; Wang, P.; Gong, W.; Xue, M.; Zhang, H.; Liu, T.; Liu, B.; Yi, Y.; Zhang, W. Bioactive polyoxygenated steroids from the South China Sea soft coral, *Sarcophyton* sp. *Mar. Drugs* **2013**, *11*, 775–787. [[CrossRef](#)]
6. Chen, W.-T.; Liu, H.-L.; Yao, L.-G.; Guo, Y.-W. 9,11-Secosteroids and polyhydroxylated steroids from two South China Sea soft corals *Sarcophyton trocheliophorum* and *Sinularia flexibilis*. *Steroids* **2014**, *92*, 56–61. [[CrossRef](#)]
7. Ngoc, N.T.; Hanh, T.T.H.; Quang, T.H.; Cuong, N.X.; Nam, N.H.; Thao, D.T.; Thung, D.C.; Kiem, P.V.; Minh, C.V. Polyhydroxylated steroids from the Vietnamese soft coral *Sarcophyton ehrenbergi*. *Steroids* **2021**, *176*, 108932. [[CrossRef](#)]
8. Wang, C.-Y.; Chen, A.-N.; Shao, C.-L.; Li, L.; Xu, Y.; Qian, P.-Y. Chemical constituents of soft coral *Sarcophyton infundibuliforme* from the South China Sea. *Biochem. Syst. Ecol.* **2011**, *39*, 853–856. [[CrossRef](#)]
9. Huang, T.-Y.; Huang, C.-Y.; Chen, S.-R.; Weng, J.-R.; Tu, T.-H.; Cheng, Y.-B.; Wu, S.-H.; Sheu, J.-H. New hydroquinone monoterpenoid and cembranoid-related metabolites from the soft coral *Sarcophyton tenuispiculatum*. *Mar. Drugs* **2021**, *19*, 8. [[CrossRef](#)]
10. Anjaneyulu, A.S.R.; Murthy, M.V.R.K.; Gowri, P.M.; Venugopal, M.; Laatsch, H. A rare prostaglandin from the soft coral *Sarcophyton crassocaule* of the Indian Ocean. *J. Nat. Prod.* **2000**, *63*, 1425–1426. [[CrossRef](#)]
11. Cheng, Z.-B.; Deng, Y.-L.; Fan, C.-Q.; Han, Q.-H.; Lin, S.-L.; Tang, G.-H.; Luo, H.-B.; Yin, S. Prostaglandin derivatives: Nonaromatic phosphodiesterase-4 inhibitors from the soft coral *Sarcophyton ehrenbergi*. *J. Nat. Prod.* **2014**, *77*, 1928–1936. [[CrossRef](#)] [[PubMed](#)]

12. Cheng, S.-Y.; Wen, Z.-H.; Chiou, S.-F.; Tsai, C.-W.; Wang, S.-K.; Hsu, C.-H.; Dai, C.-F.; Chiang, M.Y.; Wang, W.-H.; Duh, C.-Y. Ceramide and cerebrosides from the octocoral *Sarcophyton ehrenbergi*. *J. Nat. Prod.* **2009**, *72*, 465–468. [[CrossRef](#)] [[PubMed](#)]
13. Eltahawy, N.A.; Ibrahim, A.K.; Radwan, M.M.; Zaitone, S.A.; Gomaa, M.; ElSohly, M.A.; Hassanean, H.A.; Ahmed, S.A. Mechanism of action of antiepileptic ceramide from Red Sea soft coral *Sarcophyton auritum*. *Bioorg. Med. Chem. Lett.* **2015**, *25*, 5819–5824. [[CrossRef](#)] [[PubMed](#)]
14. Řezanka, T.; Dembitsky, V.M. γ -Lactones from the soft corals *Sarcophyton trocheliophorum* and *Lithophyton arboreum*. *Tetrahedron* **2001**, *57*, 8743–8749. [[CrossRef](#)]
15. Shaaban, M.; Ghani, M.A.; Issa, M.Y. New naturally occurring compounds from *Sarcophyton trocheliophorum*. *Biointerface Res. App. Chem.* **2022**, *12*, 2285–2331. [[CrossRef](#)]
16. Rodrigues, I.G.; Miguel, M.G.; Mnif, W. A brief review on new naturally occurring cembranoid diterpene derivatives from the soft corals of the genera *Sarcophyton*, *Simularia*, and *Lobophytum* since 2016. *Molecules* **2019**, *24*, 781. [[CrossRef](#)]
17. Shaaban, M.; Yassin, F.Y.; Soltan, M.M. Calamusins J-K: New anti-angiogenic sesquiterpenes from *Sarcophyton glaucum*. *Nat. Prod. Res.* **2021**, *35*, 5720–5731. [[CrossRef](#)]
18. Sawant, S.S.; Youssef, D.T.A.; Sylvester, P.W.; Wali, V.; Sayed, K.A.E. Antiproliferative sesquiterpenes from the Red Sea soft coral *Sarcophyton glaucum*. *Nat. Prod. Commun.* **2007**, *2*, 117–119. [[CrossRef](#)]
19. Anjaneyulu, A.S.R.; Rao, V.L.; Sastry, V.G.; Rao, D.V. Trocheliophorin: A novel rearranged sesquiterpenoid from the Indian Ocean soft coral *Sarcophyton trocheliophorum*. *J. Asian Nat. Prod. Res.* **2008**, *10*, 597–601. [[CrossRef](#)]
20. Ye, F.; Li, J.; Wu, Y.; Zhu, Z.-D.; Mollo, E.; Gavagnin, M.; Gu, Y.-C.; Zhu, W.-L.; Li, X.-W.; Guo, Y.-W. Sarinacetamides A and B, nitrogenous diterpenoids with tricyclo [6.3.1.0¹⁻⁵] dodecane scaffold from the South China Sea soft coral *Sarcophyton infundibuliforme*. *Org. Lett.* **2018**, *20*, 2637–2640. [[CrossRef](#)]
21. Lin, K.-H.; Lin, Y.-C.; Huang, C.-Y.; Tseng, Y.-J.; Chen, S.-R.; Cheng, Y.-B.; Hwang, T.-L.; Wang, S.-Y.; Chen, H.-Y.; Dai, C.-F.; et al. Cembranoid-related diterpenes, novel secoditerpenes, and an unusual bisditerpene from a Formosan soft coral *Sarcophyton tortuosum*. *Bull. Chem. Soc. Jpn.* **2021**, *94*, 2774–2783. [[CrossRef](#)]
22. Bu, Q.; Yang, M.; Yan, X.-Y.; Yao, L.-G.; Guo, Y.-W.; Liang, L.-F. New flexible cembrane-type macrocyclic diterpenes as TNF- α inhibitors from the South China Sea soft coral *Sarcophyton mililatensis*. *Int. J. Biol. Macromol.* **2022**, *222*, 880–886. [[CrossRef](#)] [[PubMed](#)]
23. Wang, C.; Zhang, J.; Shi, X.; Li, K.; Li, F.; Tang, X.; Li, G.; Li, P. Sarcoeleganolides C–G, five new cembranes from the South China Sea soft coral *Sarcophyton elegans*. *Mar. Drugs* **2022**, *20*, 574. [[CrossRef](#)] [[PubMed](#)]
24. Mohamed, T.A.; Elshamy, A.I.; Abd El-Razek, M.H.; Abdel-Tawab, A.M.; Ali, S.K.; Aboelmagd, M.; Suenaga, M.; Pare, P.W.; Umeyama, A.; Hegazy, M.-E.F. Sarcoconvolutums F and G: Polyoxygenated cembrane-type diterpenoids from *Sarcophyton convolutum*, a Red Sea soft coral. *Molecules* **2022**, *27*, 5835. [[CrossRef](#)]
25. Sun, P.; Cai, F.-Y.; Lauro, G.; Tang, H.; Su, L.; Wang, H.-L.; Li, H.H.; Mándi, A.; Kurtán, T.; Riccio, R.; et al. Immunomodulatory biscembranoids and assignment of their relative and absolute configurations: Data set modulation in the density functional theory/nuclear magnetic resonance approach. *J. Nat. Prod.* **2019**, *82*, 1264–1273. [[CrossRef](#)] [[PubMed](#)]
26. Li, Y.; Li, S.; Cuadrado, C.; Gao, C.; Wu, Q.; Li, X.; Pang, T.; Daranas, A.H.; Guo, Y.; Li, X. Polyoxygenated anti-inflammatory biscembranoids from the soft coral *Sarcophyton tortuosum* and their stereochemistry. *Chin. Chem. Lett.* **2021**, *32*, 271–276. [[CrossRef](#)]
27. Yan, X.; Liu, J.; Huang, J.; Wang, Y.; Leng, X.; Li, T.; Ouyang, H.; Yan, X.; He, S. Bistochelides H–L: Biscembranoids from the South China Sea soft coral *Sarcophyton serenei*. *Phytochemistry* **2022**, *204*, 113438. [[CrossRef](#)]
28. Nguyen, N.B.; Chen, L.-Y.; Chen, P.-J.; El-Shazly, M.; Hwang, T.-L.; Su, J.-H.; Su, C.-H.; Yen, P.-T.; Peng, B.-R.; Lai, K.-H. MS/MS molecular networking unveils the chemical diversity of biscembranoid derivatives, neutrophilic inflammatory mediators from the cultured soft coral *Sarcophyton trocheliophorum*. *Int. J. Mol. Sci.* **2022**, *23*, 15464. [[CrossRef](#)]
29. Al-Footy, K.O.; Alarif, W.M.; Asiri, F.; Aly, M.M.; Ayyad, S.-E.N. Rare pyrane-based cembranoids from the Red Sea soft coral *Sarcophyton trocheliophorum* as potential antimicrobial–antitumor agents. *Med. Chem. Res.* **2015**, *24*, 505–512. [[CrossRef](#)]
30. Mohamed, T.A.; Elshamy, A.I.; Abdel-Tawab, A.M.; AbdelMohsen, M.M.; Ohta, S.; Pare, P.W.; Hegazy, M.-E.F. Oxygenated cembrene diterpenes from *Sarcophyton convolutum*: Cytotoxic sarcoconvolutum A–E. *Mar. Drugs* **2021**, *19*, 519. [[CrossRef](#)]
31. Li, J.-F.; Zeng, Y.-B.; Li, W.-S.; Luo, H.; Zhang, H.-Y.; Guo, Y.-W. Xishaglaucumins A–J, new cembranoids with anti-inflammatory activities from the South China Sea soft coral *Sarcophyton glaucum*. *Chin. J. Chem.* **2022**, *40*, 79–90. [[CrossRef](#)]
32. Zhang, J.; Tang, X.; Han, X.; Feng, D.; Luo, X.; Ofwegen, L.v.; Li, P.; Li, G. Sarcoglaucins A–I, new antifouling cembrane-type diterpenes from the South China Sea soft coral *Sarcophyton glaucum*. *Org. Chem. Front.* **2019**, *6*, 2004–2013. [[CrossRef](#)]
33. Badria, F.A.; Guirguis, A.N.; Perovic, S.; Steffen, R.; Müller, W.E.G.; Schröder, H.C. Sarcophytolide: A new neuroprotective compound from the soft coral *Sarcophyton glaucum*. *Toxicology* **1998**, *131*, 133–143. [[CrossRef](#)] [[PubMed](#)]
34. Du, Y.-Q.; Chen, J.; Wu, M.-J.; Zhang, H.-Y.; Liang, L.-F.; Guo, Y.-W. Uncommon capnosane diterpenes with neuroprotective potential from South China Sea soft coral *Sarcophyton boettgeri*. *Mar. Drugs* **2022**, *20*, 602. [[CrossRef](#)] [[PubMed](#)]
35. Carroll, A.R.; Copp, B.R.; Davis, R.A.; Keyzers, R.A.; Prinsep, M.R. Marine natural products. *Nat. Prod. Rep.* **2022**, *39*, 1122–1171. [[CrossRef](#)]
36. Liu, J.; Gu, Y.-c.; Su, M.-z.; Guo, Y.-w. Chemistry and bioactivity of secondary metabolites from South China Sea marine fauna and flora: Recent research advances and perspective. *Acta Pharmacol. Sin.* **2022**, *43*, 3062–3079. [[CrossRef](#)]
37. Liang, L.-F.; Kurtán, T.; Mándi, A.; Yao, L.-G.; Li, J.; Zhang, W.; Guo, Y.-W. Unprecedented diterpenoids as a PTP1B inhibitor from the Hainan soft coral *Sarcophyton trocheliophorum* Marenzeller. *Org. Lett.* **2013**, *15*, 274–277. [[CrossRef](#)]

38. Yang, M.; Li, X.-L.; Wang, J.-R.; Lei, X.; Tang, W.; Li, X.-W.; Sun, H.; Guo, Y.-W. Sarcomililate A, an unusual diterpenoid with tricyclo [11.3.0.0^{2,16}] hexadecane carbon skeleton, and its potential biogenetic precursors from the Hainan soft coral *Sarcophyton mililatensis*. *J. Org. Chem.* **2019**, *84*, 2568–2576. [[CrossRef](#)]
39. Yang, Q.-B.; Wu, Q.; Chen, J.-K.; Liang, L.-F. The soft coral *Sarcophyton trocheliophorum*: A warehouse of terpenoids with structural and pharmacological diversity. *Mar. Drugs* **2023**, *21*, 30. [[CrossRef](#)]
40. Yao, L.-G.; Zhang, H.-Y.; Liang, L.-F.; Guo, X.-J.; Mao, S.-C.; Guo, Y.-W. Yalongenes A and B, two new cembranoids with cytoprotective effects from the Hainan soft coral *Sarcophyton trocheliophorum* Marenzeller. *Helv. Chim. Acta* **2012**, *95*, 235–239. [[CrossRef](#)]
41. Chen, Z.-H.; Gao, T.-R.; Yang, M.; Yao, L.-G.; Guo, Y.-W. Further new cembranoids from the South China Sea soft coral *Sarcophyton trocheliophorum*. *Fitoterapia* **2021**, *151*, 104902. [[CrossRef](#)] [[PubMed](#)]
42. Xi, Z.; Bie, W.; Chen, W.; Liu, D.; van Ofwegen, L.; Proksch, P.; Lin, W. Sarcophyolides B–E, new cembranoids from the soft coral *Sarcophyton elegans*. *Mar. Drugs* **2013**, *11*, 3186–3196. [[CrossRef](#)] [[PubMed](#)]
43. Jia, R.; Guo, Y.-W.; Mollo, E.; Gavagnin, M.; Cimino, G. Sarcophytonolides E–H, cembranolides from the Hainan soft coral *Sarcophyton latum*. *J. Nat. Prod.* **2006**, *69*, 819–822. [[CrossRef](#)] [[PubMed](#)]
44. Liang, L.-F.; Chen, W.-T.; Li, X.-W.; Wang, H.-Y.; Guo, Y.-W. New bicyclic cembranoids from the South China Sea soft coral *Sarcophyton trocheliophorum*. *Sci. Rep.* **2017**, *7*, 46584. [[CrossRef](#)]
45. Wen, T.; Ding, Y.; Deng, Z.; van Ofwegen, L.; Proksch, P.; Lin, W. Sinulaflexiolides A–K, cembrane-type diterpenoids from the Chinese soft coral *Sinularia flexibilis*. *J. Nat. Prod.* **2008**, *71*, 1133–1140. [[CrossRef](#)]
46. Kobayashi, M.; Kondo, K.; Osabe, K.; Mitsunashi, H. Marine terpenes and terpenoids. V. Oxidation of sarcophytol A, a potent anti-tumor-promoter from the soft coral *Sarcophyton glaucum*. *Chem. Pharm. Bull.* **1988**, *36*, 2331–2341. [[CrossRef](#)]
47. Li, S.-W.; Cuadrado, C.; Yao, L.-G.; Daranas, A.H.; Guo, Y.-W. Quantum mechanical–NMR-aided configuration and conformation of two unreported macrocycles isolated from the soft coral *Lobophytum* sp.: Energy calculations versus coupling constants. *Org. Lett.* **2020**, *22*, 4093–4096. [[CrossRef](#)]
48. Raldugin, V.A.; Pleshkov, I.G.; Gatilov, Y.V.; Yaroshenko, N.I.; Salenko, V.L.; Shevtsov, S.A.; Pentegova, V.A. Photosensitized oxidation of isocembrol. VII. Products of reaction at the C₁₁ double bond. *Chem. Nat. Compd.* **1984**, *20*, 45–52. [[CrossRef](#)]

Disclaimer/Publisher’s Note: The statements, opinions and data contained in all publications are solely those of the individual author(s) and contributor(s) and not of MDPI and/or the editor(s). MDPI and/or the editor(s) disclaim responsibility for any injury to people or property resulting from any ideas, methods, instructions or products referred to in the content.